FUZZY LOGIC BASED CONTROL OF STANDALONE WIND-PV-DIESEL BASED HYBRID MICRO-GRID.

[1] SHAIK REHANA, [2] MUSUNOORU RAMU,

[1]M. Tech PG Scholar, [2]Asst.Professor,

[1,2] Dept. of Electrical and Electronics Engineering

[1,2] Quba College of Engineering and Technology, Venkatachalam, SPSR Nellore Dist., Andhra Pradesh, India.

Abstract**:** In this paper, a thorough regulator of an independent microgrid is actualized, which has three scattered age units dependent on a breeze, sun based photovoltaic exhibit and a diesel generator. The force proportion variable advance bother and watch technique is applied to accomplish most extreme force point attaching of a sunlight based photovoltaic cluster and a variable speed wind turbine coupled a lasting magnet brushless DC generator without rotor/wind speed sensors. Besides, to guarantee ideal synchronization of a diesel generator to the point of regular coupling (PCC), a control calculation is created, which depends on in-stage and quadrature units. A functioning force control dependent on corresponding necessary regulator with against windup, is utilized for voltage and recurrence guideline. The LCL channel dependent on virtual resistor, is utilized for power quality improvement at PCC. The execution of the framework is likewise tried with fluffy rationale regulator and it been seen that reaction is better with fluffy based control plot. Reenactment and test outcomes are introduced for the approval of proposed framework.

Index Terms— Standalone microgrid, solar photovoltaic array, wind turbine, diesel generator, active damping, LCL filter based virtual resistor, PCC voltage regulation, power quality improvement and PI controller with anti-windup.

1. INTRODUCTION

Numerous far off territories despite everything utilize a diesel motor based electric generator regularly known as a diesel generator (DG) [1] for their electrical vitality needs, regardless of the way that DG is exorbitant, loud and toxin [2]. The far off zones generally have immense accessibility of sustainable power sources (RES, for example, sunlight based, wind, biomass, just as hydro. Progressions in power gadgets and electrical machines, have made it conceivable to diminish the expense of vitality gave by these RES, and to decrease reliance on DG in far off regions by coordinating different RES and to shape a neighborhood electrical system called as an independent microgrid (SMG). This electric framework is a self-reasonable and off-the-matrix connect with vitality created from locally accessible sources. Inferable from the stochastic idea of different RES, the power age needs a reinforcement backing, for example, DG, on the grounds that SMG isn't associated with any traditional lattice. Notwithstanding, such mix has AC just as DC age making the control perplexing and exorbitant [3]. In this manner, research endeavors for rearranged control, cost decrease and improved execution of SMG, are accounted for in the writing [4-15]. In [4], the creators have introduced a breeze turbine (WT) and a sunlight based photovoltaic (PV) based SMG for decrease of cost and intricacy while disposing of one force converter. In [5], the control is streamlined by disposing of the landfill load, in any case, this method can't be summed up for all applications. In [6-7], two unique arrangements are introduced to guarantee continuous force in distant and confined territories by working DGs ceaselessly. This arrangement is expensive, poison and prompts helpless productivity at light loads. To upgrade the presentation of DGs, a battery vitality stockpiling (BES), WT and DGs based SMG, is introduced in [8], where DG is utilized as a crisis vitality source [9]. In this mode, the gracefully to the heap and the battery charging, is accomplished all the while.

Many exploration endeavors [10-12] have been made for an improvement in execution of SMG, for example, expanded effectiveness, improved force quality, guideline of voltage and recurrence at purpose of regular coupling (PCC). Different control approaches are additionally introduced in [13-15] for improved execution of WT and PV cluster. The normally utilized technique for most extreme force point following (MPPT) is the irritate and watch (P&O) strategy because of its effortlessness. Nonetheless, this strategy is touchy to certain climate conditions and it brings about motions close to a most extreme force point (MPP) [16]. Numerous arrangements are proposed in the writing to settle the disadvantages of P&O technique for PV exhibit, for example, factor step size P&O strategy [17] and half breed MPPT [18] or improved P&O technique dependent on sliding mode control [19]. Be that as it may, their execution continuously, turns into a test.

Concerning of WT, P&O technique and force signal criticism strategies, are generally utilized because of their straightforwardness [20-21]. It utilizes either wind speed or rotational speed sensors to gauge the ideal force.

To keep up the framework security and burden sharing between different generators in SMG, virtual impedance, recurrence hang and edge hang control, have been accounted for in the writing [11, 22-23]. Notwithstanding, these strategies endure during breakdown of at least one generators. Also, this method depends on complex multi-circle input control [24]. For the most part, the force quality in SMG is reliant on scattered age units, nearby framework attributes, controls and associated loads [25-28]. For music moderation, inactive and dynamic channels are required. With respect to, dynamic separating, numerous procedures, for example, momentary force hypothesis, simultaneous reference outline strategy, versatile control and so on., are proposed in [25], [36-38]. In these control procedures introduced in [25], traditional relative essential (PI) regulator is utilized to follow the set focuses in inward and external control circles, where the immersion wonder isn't taken on thought when the framework arrives at cutoff points of activity. This issue is explained in [31] and [34] by fortifying the PI regulator utilizing hostile to windup input. The got outcomes show palatable exhibition when the framework arrives at its restriction of activity. The new structure of PI regulator with hostile to windup proposed in [33], is compelling, nonetheless, it requires numerical model to get ideal time constants of the counter windup input.

Concerning, lessening of exchanging recurrence music, a yield channel is required. As per [28, 29], the LCL channel is savvy channel, notwithstanding, it ought to be appropriately intended to accomplish elevated level execution. The damping resistor associated in arrangement with a capacitor of the LCL-channel, builds the encumbrance in execution and the misfortunes. This issue is unraveled in [29] by coordinating an eyewitness in the control of VSC (Voltage Source Converter). This strategy is compelling yet unpredictable. In [35], the intricacy of execution is illuminated by extra channel capacitor current detecting, however at the expanded expense.

In this work, a SMG design dependent on three scattered age units, is introduced for guaranteeing consistent gracefully to a far off water treatment station in north of Canada. A control plot for WT-PV-DG based SMG is intended to accomplish continuous nonstop force with most extreme RES investment under differing climate and burden conditions. The noteworthy commitments in this work, are as per the following.

- A SMG setup is determined with decreased force converters dependent on WT, PV cluster and DG.
- another dynamic force control system depends on a PI regulator with against windup regulator (AWPI) and ideal time steady for voltage and recurrence guideline at PCC.
- The force proportion variable advance based P&O technique is actualized to achieve elevated level execution from WT without detecting the rotor or wind speed and for PV exhibit with less motions around most extreme point under consistent state condition.
- A nitty gritty numerical model is introduced to plan precisely the boundaries of the counter windup input.
- The assessment of a virtual resistor term, is made by increasing a consistent with assessed channel capacitor current rather than detected current as it has been proposed in [35].
- The DG is utilized uniquely as reinforcement vitality source.
- A straightforward synchronization control of DG at PCC dependent on in-stage and quadrature joins layouts, is utilized.
- A financially savvy LCL-channel dependent on virtual resistor, is utilized for sounds moderation without misfortunes...

II. SYSTEM CONFIGURATION AND OPERATION MODES

The proposed SMG setup [30], which includes a perpetual magnet brushless DC generator driven by WT and a diesel motor driven coordinated generator (SG), is appeared in Fig.1. The WT is worked at variable paces, while, the simultaneous generator is worked at a fixed speed. For straightforward mix of various scattered producing units with simple synchronization, the force from WT is redressed utilizing a diode connect rectifier and took care of to the DC-interface utilizing a lift converter 2. The PV exhibit is associated with a similar DC-interface through a lift converter 1. The joined DC power is taken care of to the PCC through a three-stage VSC. A controlled switch is utilized to associate DG at PCC. The SMG arrangement is strengthened by a battery bank as BES and a DC dump burden to forestall the BES cheating. For sounds moderation at PCC, the LCL channel based virtual resistor, is utilized. To ensure a galvanic seclusion among PCC and rest of the framework, a delta-star transformer, is utilized.

In Table I, all working methods of the framework, are introduced. In light of the condition of charge of battery (SOC), the created power from WT and PV cluster, just as the heap power request, the choice is taken. In the event that the SOC is more noteworthy than half and the created power from WT and PV cluster, is more prominent than the heap request, BES is in charging mode. For the equivalent SOC yet with less force created from WT and PV, BES begins releasing for example taking care of capacity to the heap so as to adjust the force in the framework. DG is killed as it is referenced in a working mode 5, just if the SOC is under half, and the produced power from WT and PV exhibit, is not as much as burden power request. In this working mode DG runs at its full limit, to charge BES and flexibly the heap, at the same time. The DC dump load works in mode 4, just if BES is completely energized, and the created power from WT and PV cluster, is more noteworthy than the heap request..

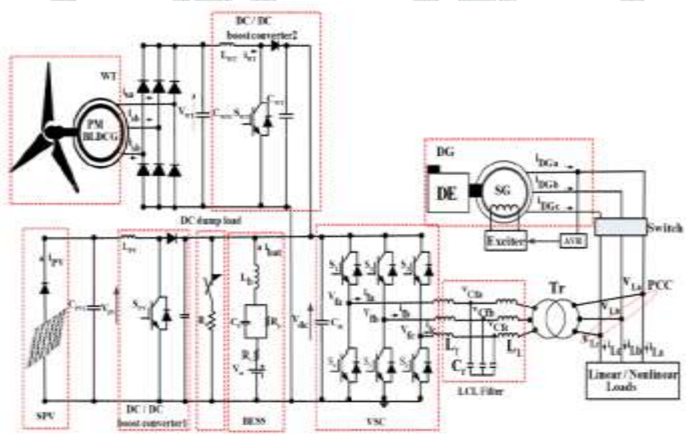

Fig.1 SMG configuration under study

TABLE I OPERATING MODES OF SYSTEM

OPERATING MODES OF SYSTEM

Mode	Conditions	Energy source	State of BES
Mode1	SOC >50% $P_{pv}+P_{WT}>P_L$	PV, WT, BES	BES is charging
Mode2	SOC >50% $P_{pv}+P_{WT}<P_L$	PV, WT, BES	BES is discharging
Mode3	SOC <50% $P_{pv}+P_{WT}>P_L$	PV, WT, BES	BES is charging
Mode4	SOC =100% $P_{pv}+P_{WT}>P_L$	PV, WT , DC dump load is turned ON	charging stopped
Mode5	SOC <50% $P_{pv}+P_{WT}<P_L$	PV, WT, BES, DG is turned ON	BES is charging

.

III. CONTROLLER DESIGN FOR SMG

The proposed SMG utilizes different regulators for acquiring wanted execution in particular MPPT, DC dump load control, DG control, voltage control and force quality improvement. In this area, the plan of control calculations, are examined.

A. Control strategy for Wind turbine

Fig.2 presents the proposed control calculation for MPPT of WT. The stator of perpetual magnet brushless DC generator is associated with the DC transport through a three-stage diode-extension and lift converter 2 to get DC voltage from trapezoidal AC voltage. This evades the rotor or wind speed sensors. The DC connect likewise has BES and watches varieties in DC interface voltage with the adjustment in wind speed for example speed of WT. Consequently, DC current (iWT) and voltage (VWT), both are essential to accomplish MPPT. In like manner, a force proportion with variable advance size-based P&O technique, is utilized to acknowledge MPPT from WT. As introduced in Fig.2, the momentary force produced from WT at nth moment, is determined utilizing the detected (iWT) and the yield voltage (vWT) at the three-stage diode-connect yield as,,

$$P_{WT(n)} = V_{WT(n)} i_{WT(n)} \quad (1)$$

The WT instantaneous power at (n-1)th instant, is obtained as,

$$P_{WT(n-1)} = V_{WT(n-1)} i_{WT(n-1)} \quad (2)$$

where PWT(n), PWT(n-1), VWT(n), VWT(n-1) and iWT(n), iWT(n-1) mean the momentary force created from WT, the deliberate yield voltage and current at out of a three-stage diode connect, and their past qualities. The variety of immediate force at nth moment is as,,

$$\Delta P_{WT(n)} = P_{WT(n)} - P_{WT(n-1)} \quad (3)$$

where ΔPWT (n) means the change in momentary created power from WT at nth moment..
The variable power ratio is calculated as,

$$S_{WT(n)} = (P_{WTmax} - P_{WT(n)})/P_{WT(n)} \quad (4)$$

where SWT(n), PWTmax represent the variable power ratio and the maximum power generated from WT.
The perturbation for the next step (KΔdWT(n)) is obtained as,

$$K\Delta d_{WT(n)} = S_{WT(n)} * \Delta T_{WT} \quad (5)$$

where ΔTWT is a step size and K denotes a gain, which is to,

$$\begin{cases} K = 1 \ if \quad \Delta P_{WT(n)} < 1 \\ K = -1 \ if \quad \Delta P_{WT(n)} > 1 \end{cases} \quad (6)$$

The control signal (dWT(n)), is expressed as,

$$d_{WT(n)} = d_{WT(n)} + K\Delta d_{WT(n)} \quad (7)$$

The control signal is taken care of to beat with tweak (PWM) square to door the IGBT switch (SWT) of a lift converter 2.

B. Control Strategy for Solar Photovoltaic Array

To move towards MPP without motions around MPP, variable advance force proportion P&O techniques is utilized. As represented in Fig.3, the immediate force created from PV exhibit is acquired from its detected yield voltage and current as,

$$P_{PV(n)} = V_{PV(n)} i_{PV(n)} \quad (8)$$

where PPV(n), VPV(n), and iPV(n) denote the instantaneous power of PV, and output voltage and current at nth instant. The pervious instantaneous power of PV array is as,

$$P_{PV(n-1)} = V_{PV(n-1)} i_{PV(n-1)} \quad (9)$$

where PPV(n-1), VPV(n-1), and iPV(n-1) denote instantaneous power of PV array, and output voltage and current at (n-1)th instant. The change in instantaneous power, is obtained as,

$$\Delta P_{PV(n)} = P_{PV(n)} - P_{PV(n-1)} \quad (10)$$

where ΔPPV (n) is a change in instantaneous generated power. The perturbation for the next step is obtained as,

$$K\Delta d_{PV(n)} = S_{PV(n)} \Delta T_{PV} \quad (11)$$

Where ΔdPV(n), ΔTPV, SPV(n), and K are the perturbation for the next step, step size, power ratio, and gain, respectively. The gain depends on the instantaneous power variation as,

$$\begin{cases} K = 1 \ if \quad \Delta P_{PV(n)} < 1 \\ K = -1 \ if \quad \Delta P_{PV(n)} > 1 \end{cases} \quad (12)$$

The power ratio is calculated as,

$$S_{PV(n)} = (P_{PVmax} - P_{PV(n)})/P_{PV(n)} \quad (13)$$

where PPVmax is maximum power generated from PV array. The control signal (dPV(n)) is expressed as,

$$d_{PV(n)} = d_{PV(n)} + K\Delta d_{PV(n)} \quad (14)$$

The control signal is fed to pulse-with modulation (PWM) block to gate the IGBT switch (SPV) of a boost converter 1.

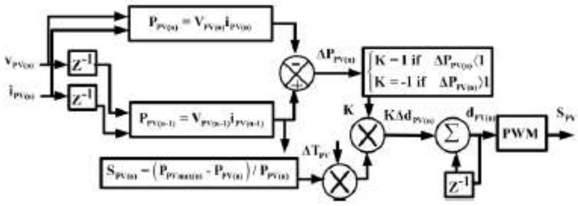

Fig. 3. Control scheme for MPPT from PV

C. Control of DC Dump Load

As appeared in Fig.1, independent microgrid is strengthened by a DC dump load associated with the DC-connection to shield BES from cheating and to forestall weakening of the force quality at PCC. The control plot for DC dump load, is introduced in Fig.4. It actuates just if BES is completely energized as itemized in Table 1 (working mode 4). The control utilizes DC interface voltage detected as the battery voltage (vdc) and its reference esteem for example the restriction of charging of battery (Vbat*) to get the voltage mistake (e). This voltage blunder (e) is gone through an AWPI regulator and the yield is the obligation proportion (dd) [31], as,,

$$d_d = \left(k\tau_C\left(\tau_i s+1\right)/\tau_i\left(\tau_C s+1\right)\right)e+\left(1/\left(\tau_C s+1\right)\right)d_{\max} \tag{15}$$

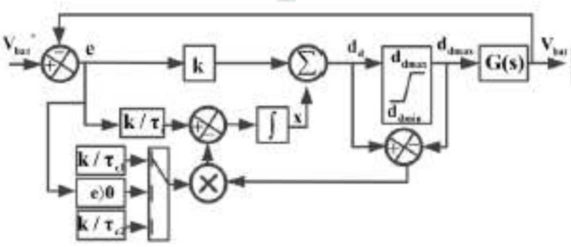

Fig. 4. DC dump load control algorithm based on AWPI

where dmax τc, τi, and k denote the maximum duty ratio, time constants and controller gain, respectively.

1) Design of Time Constants of Anti-Windup Feedback

As already indicated that anti-windup PI controller (As of now demonstrated that enemy of windup PI regulator (AWPI) is utilized to accomplish the ideal exhibition without immersion during drifters, just as, in consistent state conditions. This structure of regulator is utilized to manage BES voltage as nitty gritty in Fig.4, and to direct the PCC voltage and the yield channel current in external and inward control circles for threephase VSC. In any case, to accomplish improved execution during progress without immersion issue, ideal additions (τc, τi,), are required. To choose these ideal additions, exact numerical model for AWPI regulator is created here. The consistent state yield, dd is utilized to choose the ideal estimation of additions. Thinking about dd >ddmax, following connections are determined to get the consistent state and dynamic practices of the AWPI regulator when immersion happens. On the off chance that the yield of integrator is x, at that point;;

$$\begin{cases} dx \setminus dt = (k \setminus \tau_i)e - \left(d_d - d_{d\max}\right)(k \setminus \tau_C) \\ d_d = ke + x \end{cases} \tag{16}$$

Resulting as,

$$(dx \setminus dt) = (k \setminus \tau_i)e - (ke + x - d_{d\max})(k \setminus \tau_c) \tag{17}$$

$$(dx \setminus dt) = (k \setminus \tau_i)e - (k^2 e \setminus \tau_c) - (k \setminus \tau_c)x + d_{\max}(k \setminus \tau_c) \tag{18}$$

$$(dx \setminus dt) + (k \setminus \tau_c)x = (k \setminus \tau_i)e - (k^2 e \setminus \tau_c) + d_{d\max}(k \setminus \tau_c) \tag{19}$$

It is represented as,

This connection (19) is first request differential condition. In this way, for the dynamic conduct (comparing the variety to zero), the arrangement is acquired as,,

$$(dx \setminus dt) + (k \setminus \tau_c)x = 0 \Rightarrow (dx \setminus dt) = -(k \setminus \tau_c)xdt \tag{20}$$

In addition, the functional form of the naturel solution is as,

$$x_n\left(t\right) = Ae^{-(k \setminus \tau_c)t} \tag{21}$$

In addition, for a consistent express, the blunder e is considered as E (Error in consistent state), bringing about the got arrangement as,,

$$(k \setminus \tau_c)x_p = (k \setminus \tau_i)E - (k^2 \setminus \tau_c)E + (k \setminus \tau_c)d_{d\max} \tag{22}$$

and

$$\begin{cases} x_p = \left((k / \tau_i) E - (k^2 / \tau_c) E + (k / \tau_c) d_{d\max} \right) (\tau_c / k) \\ x_p = (\tau_c / \tau_i) E - kE + d_{d\max} \end{cases} \tag{23}$$

For general solution, the obtained expression is presented as,

$$x(t) = x_n(t) + x_p \tag{24}$$

And

$$x(t) = Ae^{-(k \backslash \tau_c)t} + (\tau_c / \tau_i) E - kE + d_{d\max} \tag{25}$$

The use of initial condition (t=0, x=X0) results,

$$\begin{cases} X_0 = A + (\tau_c / \tau_i) E - kE + d_{d\max} \\ A = X_0 - (\tau_c / \tau_i) E + kE - d_{d\max} \end{cases} \tag{26}$$

Substituting (25) in (24), it gives,

$$x(t) = \left(X_0 - \overbrace{\left(\left(\frac{\tau_c}{\tau_i} \right) - k \right)}^{D_d} E - d_{d\max} \right) Ae^{-(k/\tau_c)t} + \overbrace{\left(\left(\frac{\tau_c}{\tau_i} \right) - k \right)}^{D_d} E + d_{d\max}$$

The output for the steady state operation is given as,

$$D_d = \left((\tau_c \backslash \tau_i) - k \right) \tag{28}$$

Hence, to keep away from the immersion, Dd must be negative if the blunder is positive and positive if the mistake is negative. That is to say,,

$$\begin{cases} \text{if } E \rangle 0, \ (\tau_c / \tau_i) - k \langle 0 \Rightarrow (\tau_c / \tau_i) \langle k \\ \text{if } E \langle 0, \ (\tau_c / \tau_i) - k \rangle 0 \Rightarrow (\tau_c / \tau_i) \rangle k \end{cases} \tag{29}$$

To dodge immersion issue and accomplish superior whenever, the time constants and regulator gain, τc1, τc2, τi, and k are chosen equivalent to 3, 0.5, 10 and 2, separately..

D. Control of DG Synchronizer Switch

Fig.5 outlines the control conspire for DG synchronizer switch. Its model incorporates a speed controller, actuator, and a motor as mechanical parts and the simultaneous generator, exciter and programmed voltage controller (AVR) as electrical parts. Extra data on this numerical model might be acquired from [24]. As referenced in Table I in working mode 5 that DG in this framework carries on as a crisis vitality source and it works just if the produced power from WT and PV exhibit, is not as much as burden power request and the SOC of BES is under half. To work DG effectively, charging BES and providing the heap is done all the while. With respect to, synchronization of DG to PCC, following conditions ought to be fulfilled.

$$\begin{cases} SOC\% \langle 50\% \\ P_{PV} + P_{WT} \langle P_L \\ \theta_{DG} = \theta_L \\ V_{DGP} = V_{LP} \end{cases} \tag{30}$$

where, SOC%, PL, PPV, PWT, θDG, θL, VDGP, and VLP indicate the SOC of BES, load request, produced power from PV cluster and WT, stage point of terminal voltage of simultaneous enerator and PCC, just as, their voltage amplitudes, separately..

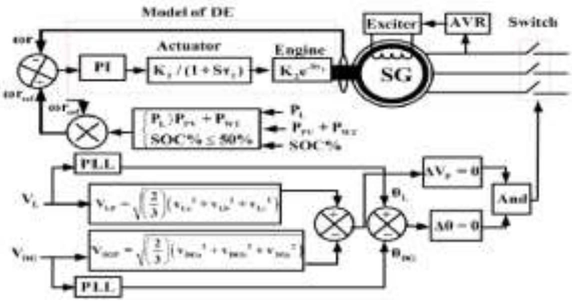

Fig. 5. Control scheme for DG synchronizer switch

The stage bolted circle (PLL) used to ascertain the stage edge of terminal voltage of simultaneous generator and PCC, depends on in-stage and quadrature unit layouts, given as,,

$$\left\{ u_{DGap} = \frac{v_{DGa}}{V_{DGP}}, u_{DGbp} = \frac{v_{DGb}}{V_{DGP}}, u_{DGcp} = \frac{v_{DGc}}{V_{DGP}} \right. \tag{31}$$

And

$$\begin{cases} u_{DGaq} = \left(1 \backslash \sqrt{3}\right)\left(-u_{DGbp} + u_{DGcp}\right) \\ u_{DGbq} = \left(\sqrt{3} \backslash 2\right)u_{DGap} + \left(1 \backslash 2\sqrt{3}\right)\left(u_{DGbp} - u_{DGcp}\right) \\ u_{DGcq} = -\left(\sqrt{3} \backslash 2\right)u_{DGap} + \left(1 \backslash 2\sqrt{3}\right)\left(u_{DGbp} - u_{DGcp}\right) \end{cases}$$

where uDGap, uDGbp, uDGcp, and uDGaq, uDGaq, uDGaq denote the inphase and quadrature unit templates. VDGP is the amplitude of voltage of synchronous generator, which is calculated as,

$$V_{DGP} = \sqrt{\left(\frac{2}{3}\right)\left(v_{DGa} + v_{DGb} + v_{DGc}\right)} \qquad (33)$$

Using (32) and (33), cosθDG and sinθDG are estimated as,

$$\begin{cases} \cos\theta_{DG} = u_{DGaq} \\ \sin\theta_{DG} = u_{DGap} \end{cases} \qquad (34)$$

This technique is applied to assess cosθL and sinθL at PCC.

On the off chance that conditions surrendered (30), are fulfilled, the reference rotor speed (ωref) is duplicated by 1 and contrasted and estimated rotor speed (ωr). The acquired blunder signal is taken care of to PI regulator, and the yield of PI regulator is taken care of to actuator. The yield of actuator speaks to the fuel stream, which is changed into mechanical force. DG infuses power into PCC just if states of synchronization, are fulfilled,

$$\begin{cases} \Delta_{VP} = V_{LP} - V_{DGP} = 0 \\ \Delta\theta = \theta_L - \theta_{DG} = 0 \end{cases} \qquad (35)$$

where ΔVP and Δθ indicate the adjustment in abundancy of voltages and stage edge of the coordinated generator and PCC.

E. Control of Three-Phase VSC

As appeared in Fig.6, the created dynamic force dependent on AWPI regulator with virtual resistor based dynamic damping, is utilized to manage the voltage and recurrence, just as to improve the force quality at PCC. This control system comprises of external and internal control circles in dq-outline. To accomplish elevated level execution under various conditions without immersion issue, AWPI regulators are utilized in both the control circles. To diminish the multifaceted nature and to expand the framework proficiency, the detached resistor of the yield LCL channel is taken out and supplanted by a virtual resistor. As introduced in Fig.6, voltages at PCC, load flows and yield channel flows are utilized to create reference voltages at the contribution of the LCL channel. The ideal voltages at PCC, are acquired utilizing the exchange capacity of LCL channel in dq-outline.

The numerical model of the LCL channel utilizes dq-reference outline as communicated in (36-38) [29], where the voltages and flows, detected at PCC, VSC yield, and channel capacitor, are changed over from fixed reference edge to pivoting reference outline utilizing Park change as,,

$$\begin{cases} \overbrace{L_L \frac{di_{Ld}}{dt} + R_L i_{Ld}}^{u_{Ld}} = v_{Ld} - v_{Cfd} - j\omega L_L i_{Lq} \\ \overbrace{L_L \frac{di_{Lq}}{dt} + R_L i_{Lq}}^{u_{Lq}} = v_{Lq} - v_{Cfq} + j\omega L_L i_{Ld} \end{cases} \qquad (36)$$

where LL, RL, ω, iLdq, vLdq, and vCfdq signify the inductor and resistor at PCC, recurrence at PCC, load voltages/flows in dq-casing, and voltage across channel capacitor in dq-outline..

$$\begin{cases} \overbrace{L_f \frac{di_{fd}}{dt} + R_f i_{fd}}^{u_{fd}} = v_{fd} - v_{Cfd} - j\omega L_f i_{fq} \\ \overbrace{L_f \frac{di_{fq}}{dt} + R_f i_{fq}}^{u_{fq}} = v_{fq} - v_{Cfq} + j\omega L_f i_{fd} \end{cases} \qquad (37)$$

where Lf, Rf, ω, ifdq, vfdq and vCfdq speak to the inductor and resistor at yield of VSC, recurrence at PCC, VSC voltage and current in dq-edge, and voltage over the channel capacitor in dq-outline, individually.

$$\begin{cases} C_f \frac{dv_{Cfd}}{dt} = i_{fd} - i_{Ld} - j\omega C_f v_{Cfq} \\ C_f \frac{dv_{Cfq}}{dt} = i_{fq} - i_{Lq} + j\omega C_f v_{Cfd} \end{cases} \qquad (38)$$

where Cf means the capacitor of LCL channel. The gracefully recurrence at PCC is fixed as 60 Hz.

The reverberation recurrence of LCL channel [29,32] is determined as,,

$$\omega_{res} = \sqrt{\left(L_f + L_L\right) / \left(C_f L_L L_f\right)} \qquad (39)$$

Fig. 7 shows the LCL channel with and without latent damping resistor. The exchange capacity of it appeared in Fig.7 (an) is as,

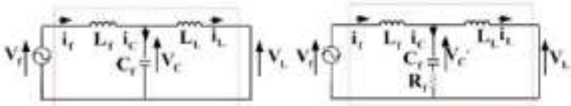

Fig. 6. LCL filter: (a) with virtual resistor, (b) with passive damping resistor

$$G_1(S) = \frac{V_C(S)}{V_f(S)} = \frac{L_L}{L_f L_L C_f S^2 + L_L + L_f} \quad (40)$$

The exchange work between the capacitor current and voltage of the LCL channel is as,

$$G_2(S) = \frac{i_C(S)}{V_C(S)} = SC_f \quad (41)$$

The exchange work when the virtual resistor based dynamic damping is presented in the AWPI regulator is as,

$$G_3(S) = \frac{V_C(S)}{V_f(S)} = \frac{L_L}{L_L L_f C_f S^2 + C_f K_r L_L S + L_f + L_L} \quad (42)$$

Appropriately, the exchange capacity of LCL channel appeared in Fig.7 (b) where damping is accomplished by detached resistor is as,,

$$G_4(S) = \frac{V_C'(S)}{V_f(S)} = \frac{L_L\left(1+SC_f R_D\right)}{L_L L_f C_f S^2 + \left(1+SC_f R_D\right)\left(L_f + L_L\right)}$$

where RD and Kr indicate the detached resistor and consistent, which is gotten utilizing (42) and (43) as,

$$K_r = R_D \frac{L_L + L_f}{L_L} \quad (44)$$

To forestall a huge VSC voltage decline, the consistent Kr ought not be excessively high. It ought to fluctuate somewhere in the range of 9 and 27, as decided in [33]. For this situation, Kr is chosen as 12.

The control system in Fig.6, comprises of external and internal control circles in dq-outline. In the external circle, the yield VSC flows in dq-outline (ifdq *) are gotten by including the yield of the AWPI regulators, which speaks to the channel capacitor flows (iC qd*) with the detected burden flows (iLdq). The terms (- ωCfvCfq and ωCfvCfd) are utilized to decouple the dq-outline.

The VSC current mistakes (Δifdq), which are contributions of the internal control circles in dq-outline, are taken care of to AWPI regulators and its yield is deducted from the terms (icdq *kr) to guarantee framework dependability without expanding the misfortunes. These terms speak to the dynamic damping, which are acquired by duplicating the assessed channel capacitor current (iCdq *) with consistent Kr surrendered (44). Besides, in inward control circles, terms (ωLfifq and - ωLfifd) are added to decouple d-q tomahawks elements. The yields of inward control circles are yield VSC voltages. In any case, reference PCC voltages in dq-outline (vLdqref) are acquired utilizing (42). These three stage PCC voltages utilizing converse Park change are taken care of to beat with tweak (PWM) square to entryway the IGBTs switches (S1-S6) of VSC..

Fuzzy control system:

A fuzzy control framework is a control framework dependent on fuzzy logic—a scientific framework that investigates simple info esteems as far as sensible factors that take on constant qualities somewhere in the range of 0 and 1, as opposed to old style or advanced logic, which works on discrete estimations of either 1 or 0 (true or false, separately). Fuzzy logic is broadly utilized in machine control. The term 'fuzzy' alludes to the way that the logic included can manage ideas that can't be communicated as the 'true' or 'false' yet rather as partially true'. Albeit elective methodologies, for example, generic calculations and neural systems can perform similarly just as fuzzy logic much of the time, fuzzy logic has the preferred position that the answer for the issue can be thrown in wording that human administrators can see, so their experience can be utilized in the structure of the controller. This makes it simpler to motorize errands that are as of now effectively performed by people.

Fuzzy sets:

The information factors in a fuzzy control framework are all in all mapped by sets of enrollment capacities like this, known as fuzzy sets. The way toward changing over a fresh information incentive to a fuzzy worth is called 'fuzzification'.

The enrollment elements of the Fuzzy controller utilized in our reproduction model are given as pursues.

a) Input 1 Membership Function:

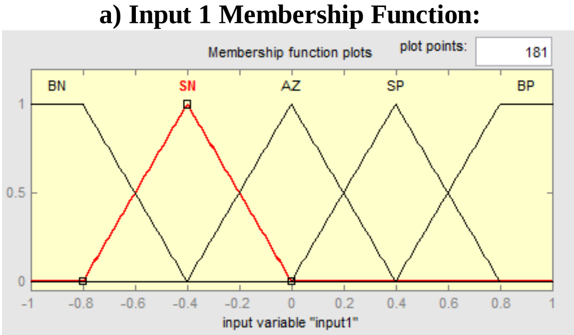

b) Input 2 Membership Function:

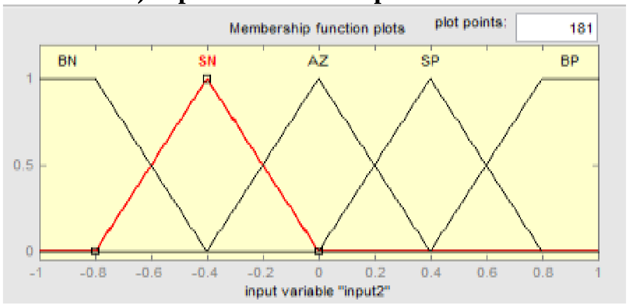

c) Output Membership Function:

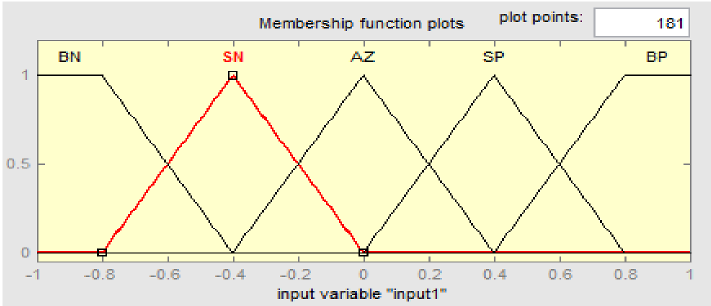

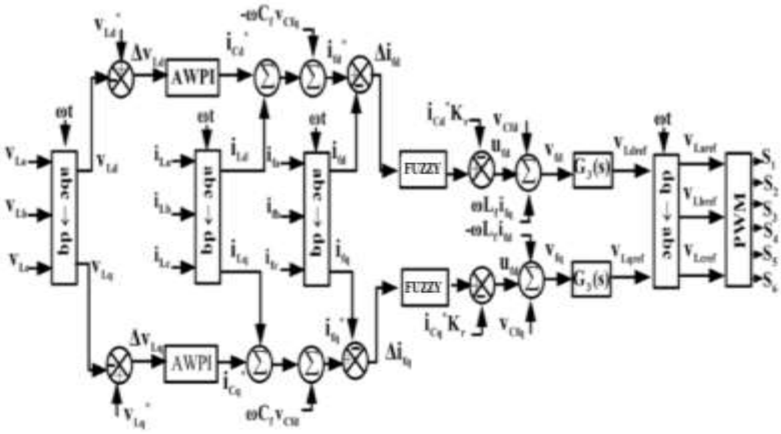

(d) fuzzy based Control algorithm for voltage regulation

Fig 9 (a) Input 1 Membership Function, (b) Input 2 Membership Function, (c) Output Membership Function, (d) FUZZYbased control scheme with active damping technique

IV. SIMULATION RESULTS:

With PI controller:

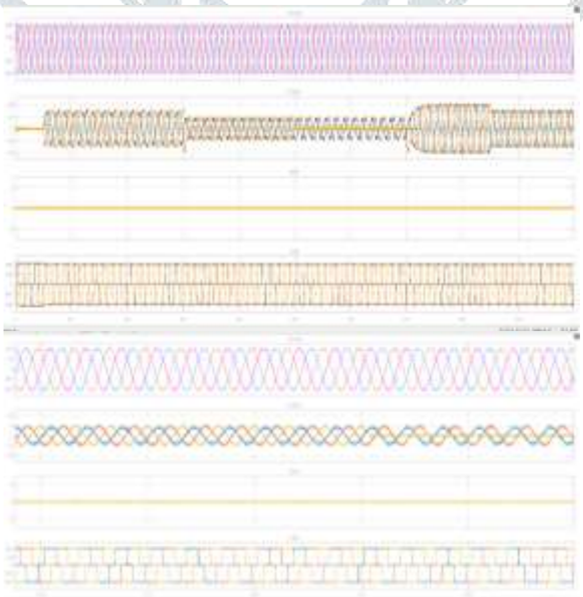

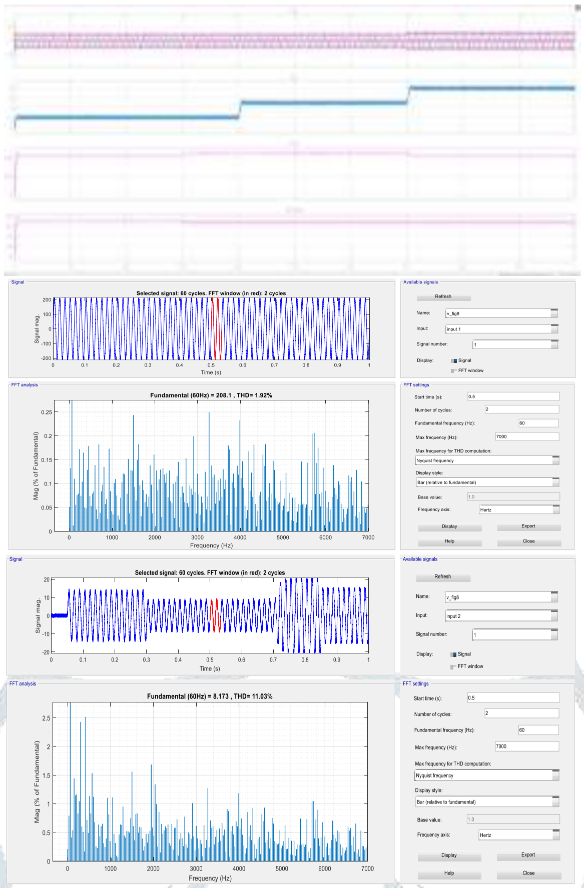

Fig.8 a) Simulation results for load and weather variation when the SOC is sperior to 50%, and b) zoomed responses of (a) between t = 0.35s and t=0.6s

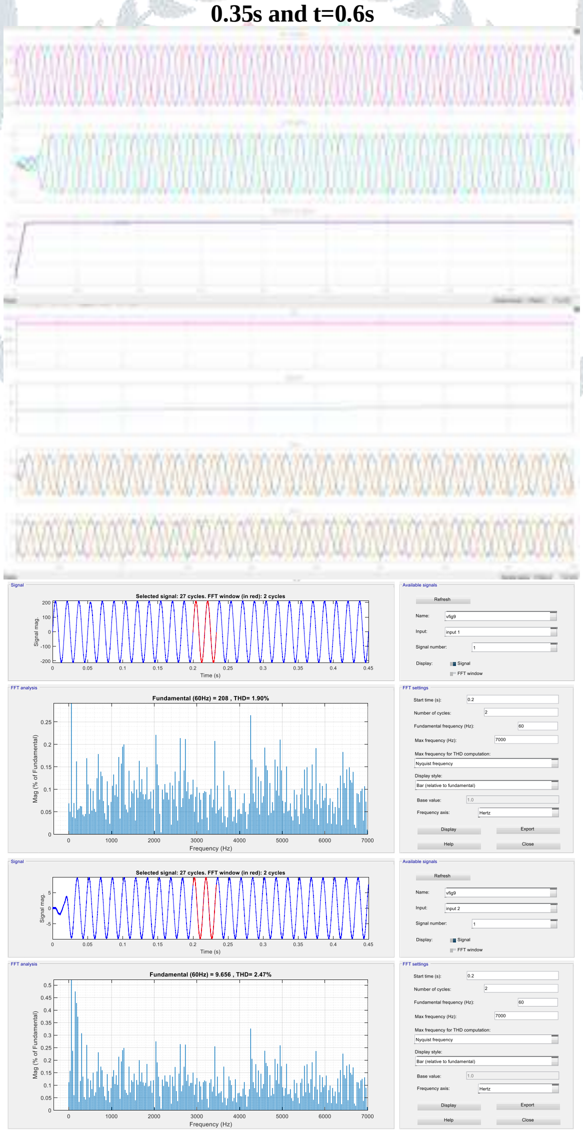

With Fuzzy controller:

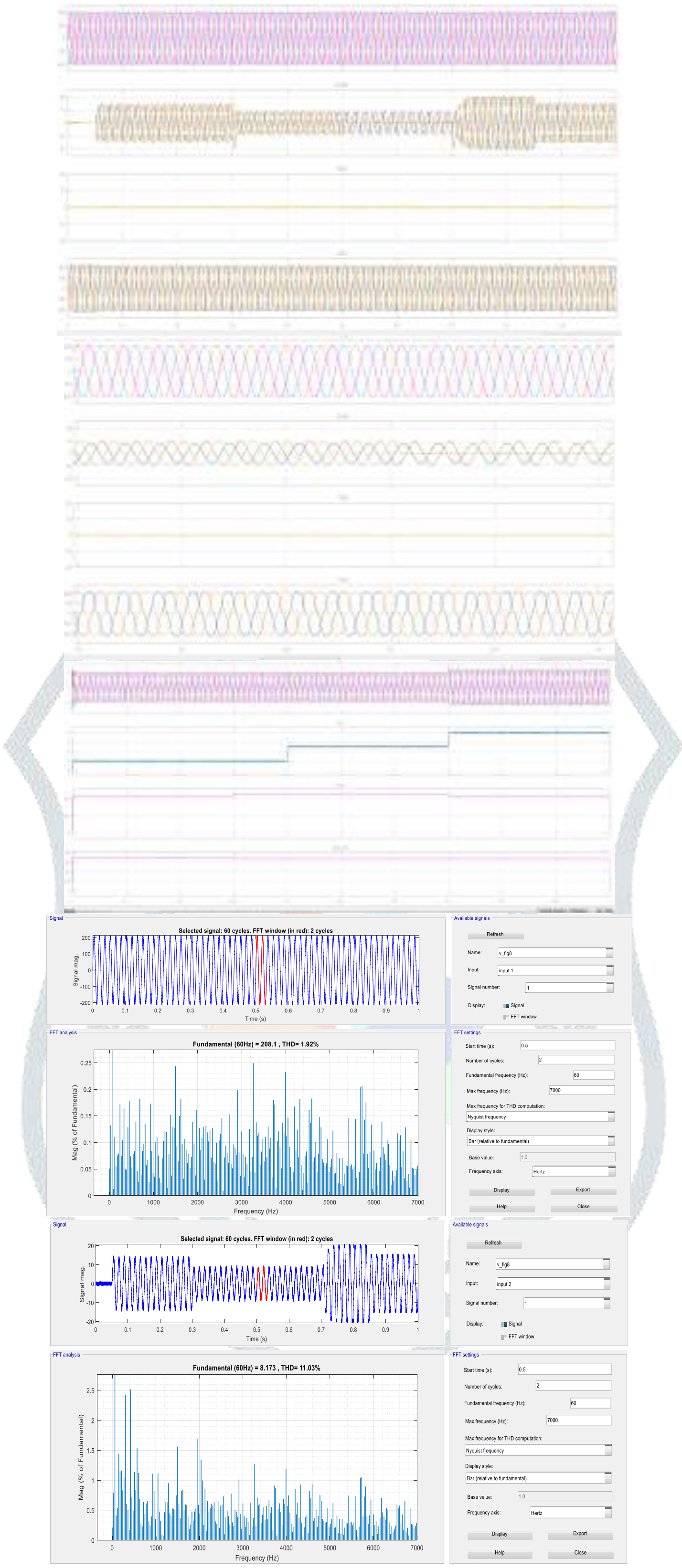

Fig.8 a) Simulation results for load and weather variation with Fuzzy Logic Controller when the SOC is sperior to 50%, and b) zoomed responses of (a) between t = 0.35s and t=0.6s

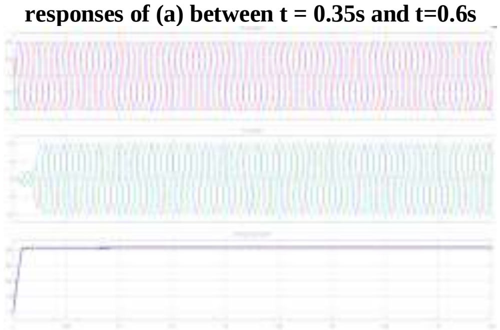

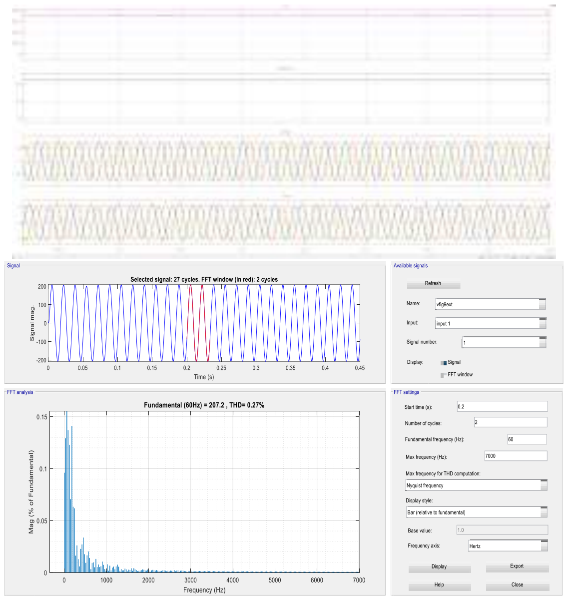

Fig.9 Dynamic performance when SOC% is less than 50%

V. CONCLUSION

The proposed microgrid for a detached water treatment station dependent on three scattered age units; fixed speed DG, variable speed wind turbine and sun oriented photovoltaic exhibit, has been found to work securely at cut off conditions while providing the heap request consistently at managed voltage. The force proportion variable advance P&O technique for MPPT, has effortlessly been actualized in a model to accomplish elevated level of execution from wind turbine and sun based photovoltaic exhibit with no wind/speed sensors and without motions around MPP. The created dynamic force control dependent on AWPI regulator with virtual resistor based dynamic damping for voltage guideline at PCC, has been actualized adequately and acquired outcomes have shown wanted execution without immersion issue during advances. The BES is shielded from cheating with use of overabundance power for space warming framework as a DC dump load. DG has been utilized distinctly as a reinforcement vitality source and its synchronization with PCC has been accomplished securely without destabilizing the framework activity. Exchanging sounds are totally lessened without misfortunes utilizing LCL channel based virtual resistor. More over the exhibition of the framework is better with fluffy rationale regulator contrasted with customary control plot. Consequently, it is presumed that the complete control proposed in this work for wind-sunlight based diesel based independent microgrid, is required to be a compelling option for continuous flexibly in distant and detached regions.

VI. REFERENCES

[1] N. Mendis, K. M. Muttaqi, S. Perera, and M. N. Uddin, “Remote Area Power Supply System: An Integrated Control Approach Based on Active Power Balance,” IEEE Industry Applications Magazine, vol.21, no.2,pp.63-76, Mar. 2015.

[2] M. Rezkallah, S. Sharma, A. Chandra and B. Singh, “Implementation and control of small-scale hybrid standalone power generation system employing wind and solar energy,” in Proc. IEEE IAS Annual Meeting, 2016.

[3] Y. Tan, K. M. Muttaqi, P. Ciufo, and L. Meegahapola, “Enhanced Frequency Response Strategy for a PMSG-Based Wind Energy Conversion System Using Ultracapacitor in Remote Area Power Supply Systems,” IEEE Trans. Industry Applications., vol.53, no.1, pp. 549-558, Feb.2017.

[4] M. Rezkallah, A. Hamadi, A. Chandra, and B. Singh, “Hybrid AC-DC standalone system based on PV array and wind turbine,” in Proc. IECON, 2014, pp. 5533-5539.

[5] M. Rezkallah, A. Hamadi, A. Chandra, and B. Singh, “Real-Time HIL Implementation of Sliding Mode Control for Standalone System Based on PV Array Without Using Dumpload,” IEEE Trans. Sustainable Energy, vol. 6, no.4, pp. 1389-1398, Oct.2015.

[6] K. Kant, C. Jain, and B. Singh, “A Hybrid Diesel-Wind-PV based Energy Generation System with Brushless Generators,” IEEE Trans.Industrials. Informatics, vol.13, no.4, pp. 1714-1722, Aug. 2017.

[7] P. Sharma and T. S. Bhatti, “Performance Investigation of Isolated Wind-Diesel Hybrid Power Systems With WECS Having PMIG,” IEEE Trans. Industrial Electronics, vol.60, no.4, pp. 1630-1637, April 2013.

[8] M. Rezkallah, A. Chandra, D. R. Rousse, H. Ibrahim, A. Ilinca, and D. Ramdenee, “Control of small-scale wind/diesel/battery hybrid standalone power generation system based on fixed speed generators for remote areas,” in Proc. IECON 2016, pp. 4060-4065.

[9] M. Rezkallah, A. Chandra, and B. Singh, "Three-leg four-wire voltage source inverters for hybrid standalone system feeding unbalanced load," in Proc. IECON, 2013, pp. 1916-1921:

[10] J. Philip, C. Jain, K. Kant, B. Singh, S. Mishra, A. Chandra, et al., “Control and Implementation of a Standalone Solar Photovoltaic Hybrid System,” IEEE Trans. Industry Applications., vol.52, no.4, pp. 3472-3479, Jul. 2016.

[11] Y. Sun, X. Hou, J. Yang, H. Han, M. Su, and J. M. Guerrero, “New Perspectives on Droop control in AC MicroGrid,” IEEE Trans. Industrial Electronics., vol.64, no.7, pp. 5741-5745, Jul. 2017.

[12] H. R. Baghaee, M. Mirsalim, G. B. Gharehpetian, and H. A. Talebi, “A Decentralized Power Management and Sliding Mode Control Strategy for Hybrid AC/DC Microgrids including Renewable Energy Resources,” Trans. Industrials. Informatics, Early Access, 2018.